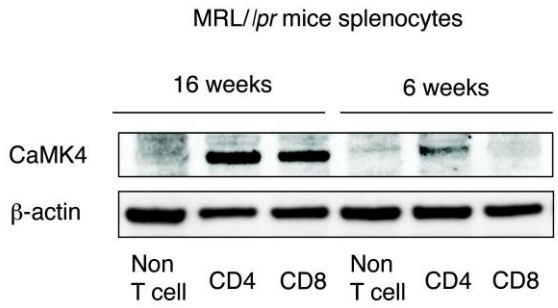

Supplementary Figure 1. CaMK4 expression is increased in T cells from MRL/*lpr* lupus-prone mice. CaMK4 was detected by western blotting in non T cell, $CD4^+$ T cell and $CD8^+$ T cell of sorted spleen cell lysates from MRL/*lpr* mice. Data are representative of 2 independent experiments with 3-4 mice per group.

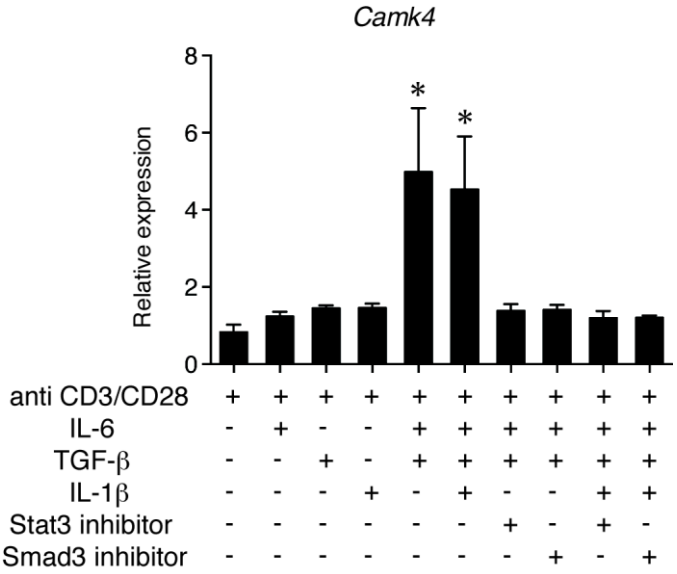

Supplementary Figure 2. Both IL6 and TGF-β are necessary for the induction of CaMK4 in T cells.

Real-time PCR analysis of *Camk4* mRNA in naive $CD4^+$ T cells from MRL/*lpr* mice stimulated by anti-CD3 and anti-CD28 antibodies for 6 hours with IL-6 alone, TGF-β alone, IL-1β alone, IL-6 + TGF-β or IL-6 + TGF-β +IL-1β in the presence or absence of STAT3 inhibitor (static; 10 M) or Smad3 inhibitor (SIS3; 10 M). Results were normalized to *Gapdh* (*$p < 0.05$; mean ± SEM; n = 4-6).

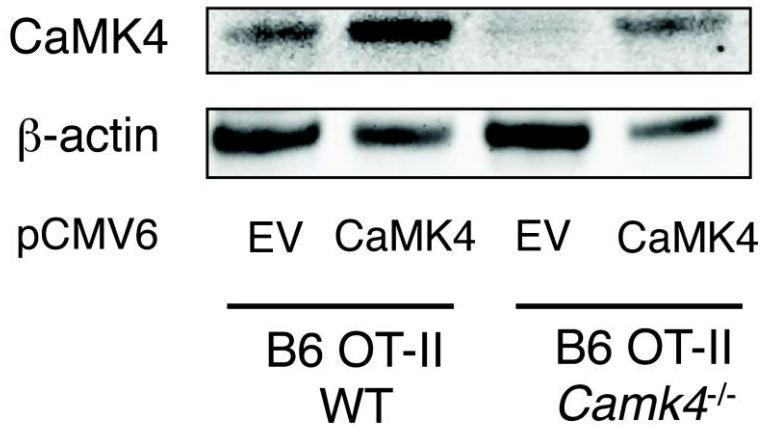

Supplementary Figure 3. CaMK4 is induced by pCMV-Camk4 vector. OT-II (WT or *Camk4*$^{-/-}$) cells were transfected with either empty vector or pCMV-Camk4. A representative image of CaMK4 expression (western blot) at 48 hr after transfection is shown. Data are representative of 2 independent experiments.

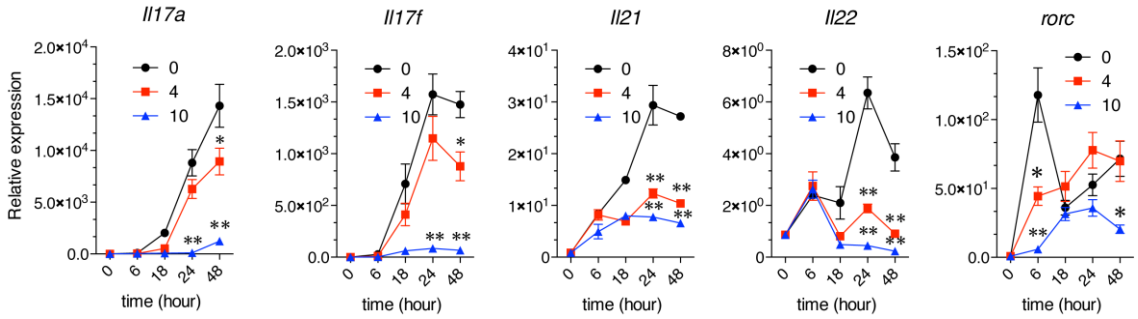

Supplementary Figure 4. KN-93 inhibits the expression of T_H17 transcription factors and T_H17 cell associated cytokines. Quantitative real-time PCR analysis of the time course of the expression of *Il17a, Il17f, Il21, IL22* and *rorgc* mRNA in naive $CD4^+$ T cells polarized into T_H17 cells in the presence of different concentrations of KN-93 (presented as in Figure 2) (*p < 0.05, **p < 0.01; mean ± SEM; n = 4-7).

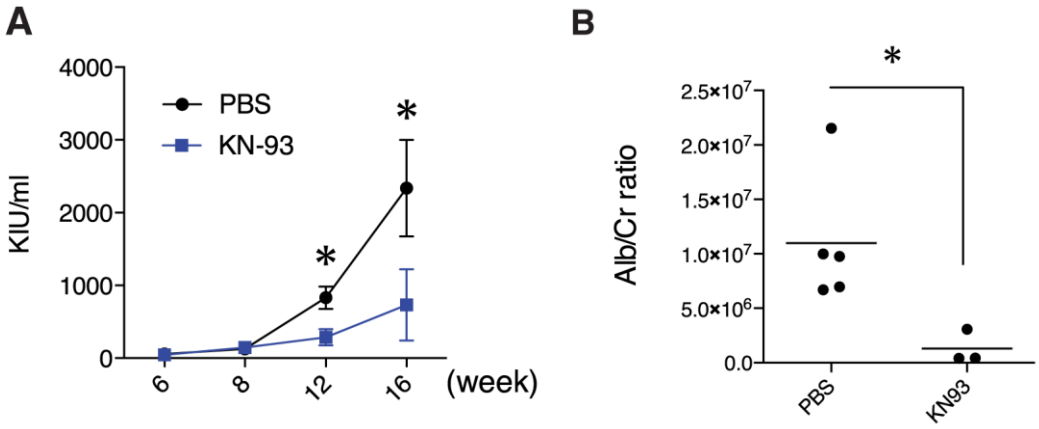

Supplementary Figure 5. Treatment of MRL/*lpr* mice with KN-93 ameliorates lupus-like disease. (A) Anti-dsDNA IgG Abs were measured in sera of MRL/*lpr* mice treated with PBS or KN-93 at the indicated time points (*$p < 0.05$; mean ± SEM; n = 4-6). (B) Proteinuria (urinary albumin/creatinine ratio) was measured at 16 weeks of age by ELISA (*$p < 0.05$). Results represent two independent experiments.

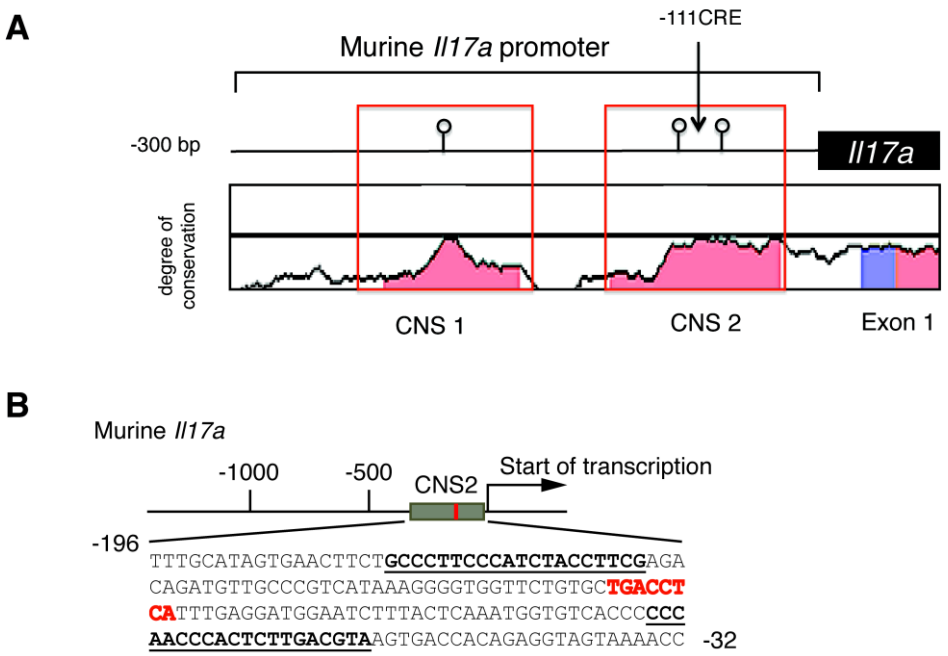

Supplementary Figure 6. Bioinformatic analysis of the *IL17a* promoters.

(A) Alignment of the mouse and human *IL17* genes are shown. Pink peaks denote CNS sites, purple peaks are exons with sequence identity of 75% over at least 200 bp. Red squares denote conserved noncoding sequences that were determined regions of interest for further analysis of DNA methylation. (B) Sequence map of murine *I17a* promoter including the CRE-binding region (red) and primers we used (bold) as described in supplementary table 1.

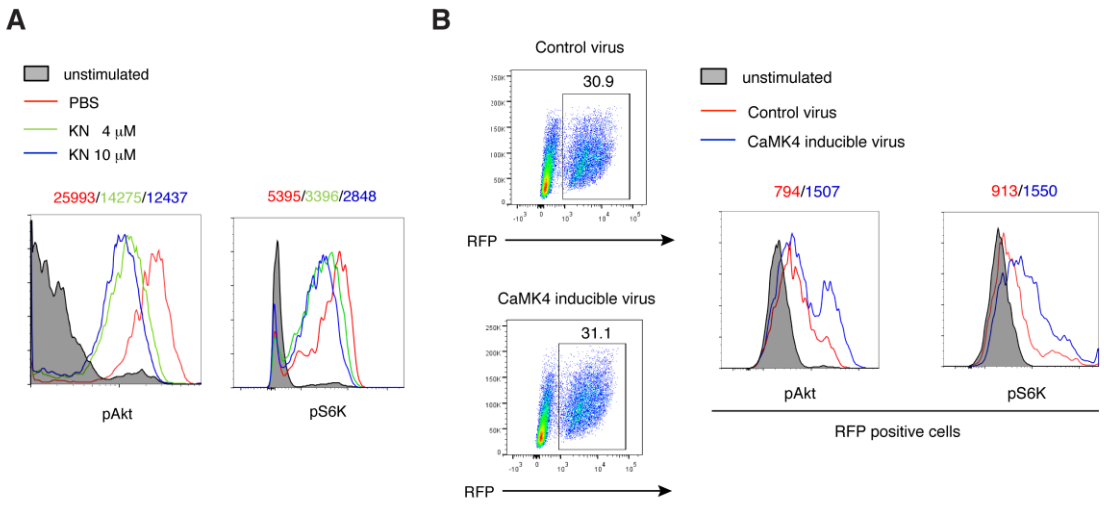

Supplementary Figure 7. CaMK4 is involved in the Akt/mTOR pathway in Jurkat T cells.

(A) Comparison of phosphorylation of Akt and S6K between PBS treated and KN-93 treated Jurkat T cells. MFI is presented above the plots. Results represent two independent experiments. (B) Jurkat T cells infected with control lentivirus or CaMK4 inducible lentivirus were gated on RFP and stained for the expression of phosphorylated Akt or S6K. MFI is presented above the plots. Results represent two independent experiments.

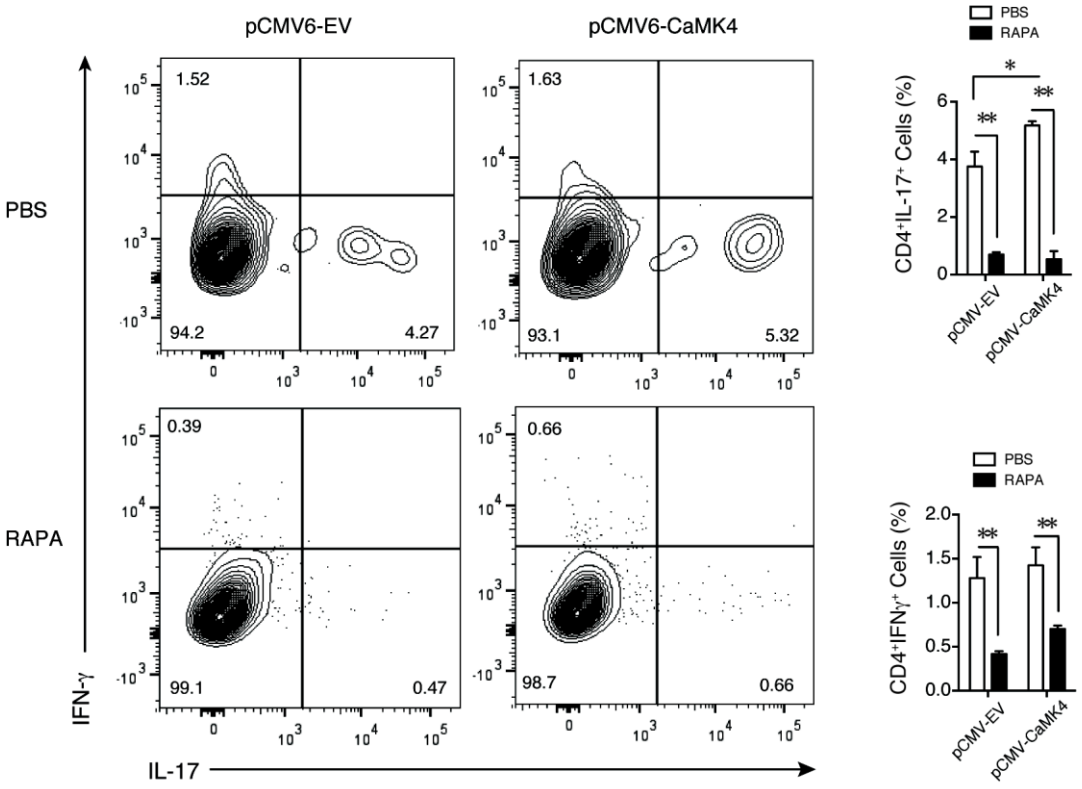

Supplementary Figure 8. CaMK4 mediated IL-17 production is blocked by rapamycin. Naïve T cells stimulated for 24 h with anti-CD3 and anti-CD28 antibodies from spleen of B6 mice were transfected with either empty vector or pCMV-Camk4. Four hours after transfection cells were stimulated under T_H17 conditions in the absence or presence of rapamycin (RAPA; 100nM). After 48 hours, IL-17 producing $TCR\beta^+CD4^+$ T cells were measured by intracellular cytokine staining. A profile representative of four mice per group is shown. Cumulative data are shown on the right side panels.

Supplementary Table 1. PCR primers

***Il17* MeDIP**	**Forward**	**Reverse**
CNS 1	ACCATTACTATGGAGCCCAGC	AGCTGAACAGAGATGCTTTGC
CNS 2	GGTGGTTCTGTGCTGACCTC	ACCTCTGTGGTCACTTACGTC
ChIP	**Forward**	**Reverse**
*Il17*_CRE-111	GCCCTTCCCATCTACCTTCG	TACGTCAAGAGTGGGTTGGG